4,15-Diamino[2.2]paracyclophane as a Starting Material for Pseudo-Geminally Substituted [2.2]Paracyclophanes[‡]

Kamal El Shaieb,[a] Vijay Narayanan,[a] Henning Hopf,*[a] Ina Dix,[a] Axel Fischer,[b] Peter G. Jones,[c] Ludger Ernst,[d] and Kerstin Ibrom[a]

Keywords: Conformational equilibrium / Cycloaddition / Cyclophanes / Hydrogen bonds / NMR spectroscopy

Diazotization of the title compound **3**, followed by treatment of the formed bis(diazonium ion) with cuprous chloride, yields the pseudo-geminal dichloride **1**. Similarly, **3** is converted into the bis(azide) **5** when sodium azide is used as the trapping nucleophile. Hypochlorite oxidation of **3** furnishes the azo compound **4**, the first multi-bridged cyclophane with a bridge consisting only of heteroatoms. Reduction of **4** with zinc/acetic acid affords the substrate **3** again. Treatment of **4** with bromine/iron powder or iodine monochloride causes deazotization accompanied by halogen introduction in pseudo-geminal position (i.e., formation of **2** and **6**, respectively). Flash vacuum pyrolysis (450 °C, 0.01 Torr) of **4** produces the phenanthrene derivatives **13** and **14**, while with tetracyanoethylene (TCNE) the azophane undergoes rapid cycloaddition at room temperature to give the [2+4] cycloadduct **16**. The structures of **1**, **2**, **4**–**6**, and **16** have been determined by X-ray structural analysis. Molecular packing patterns are determined by weak hydrogen bonds; a common packing pattern for cyclophane derivatives is ascribed to C–H···π interactions. Full bandshape analyses of the bridge proton signals in the ^{1}H NMR spectra of **1**, **2**, **6**, and of the difluoro analogue **17** yielded the vicinal ^{1}H,^{1}H coupling constants. These reflect the 1:1 equilibrium between the two skew conformations of the bridges.

Introduction

We recently described a straightforward synthesis of 4,15-diamino[2.2]paracyclophane (**3**, Scheme 1), a layered compound that may formally be regarded as a "dimer" of aniline in which the two aromatic subunits are fixed in parallel orientation by the two ethano bridges; we also showed that **3** can be used as a template molecule to carry out topochemical reactions in solution.[2] In this paper we report that the diamine is a useful precursor for the preparation of other pseudo-geminally substituted cyclophanes, including the first multi-bridged cyclophane with a bridge consisting only of heteroatoms.

[‡] Cyclophanes, LI. Part L: Ref.[1]
[a] Institut für Organische Chemie, Technische Universität Braunschweig,
Hagenring 30, 38106 Braunschweig, Germany
Fax: (internat.) + 49-(0)531/391-5388
E-mail: H.Hopf@tu-bs.de
[b] Chemisches Institut, Universität Magdeburg,
Universitätsplatz 2, 39106 Magdeburg, Germany
[c] Institut für Anorganische und Analytische Chemie, Technische Universität Braunschweig,
Postfach 3329, 38023 Braunschweig, Germany
Fax: (internat.) + 49-(0)531/391-5387
E-mail: p.jones@xray36.anchem.nat.tu-bs.de
[d] NMR-Labor der Chemischen Institute, Technische Universität Braunschweig,
Hagenring 30, 38106 Braunschweig, Germany
Fax: (internat.) + 49-(0)531/391-8192
E-mail: L.Ernst@tu-bs.de

Results and Discussion

Subjection of **3** to standard diazotization conditions (sodium nitrite, concd. hydrochloric acid) clearly converted its two amino groups into diazonium functions, since treatment of the produced intermediate with cuprous chloride and sodium azide, respectively, produced the dichloride **1** (35%) and the bis(azide) **5** (31%, Scheme 1). The structure of these two derivatives, the yields of which have not been optimized, follows from their spectroscopic data (see Exp. Sect.), especially their ^{1}H and ^{13}C NMR spectra, which are similar in their general appearance to the corresponding spectra of the substrate **3**. Furthermore, single-crystal X-ray structural analyses could be carried out for both derivatives; the results are shown and discussed below.

When **2** was oxidized with sodium hypochlorite in ethanol in the presence of base, the azo-bridged cyclophane **4** was produced in 98% yield. This triply bridged compound is the first representative of a cyclophane with a bridge consisting only of heteroatoms.[3] Again, the structure of the product follows from its spectral parameters (Exp. Sect.) as well as an X-ray crystallographic analysis (see below). On treatment with zinc in acetic acid, **4** was reduced back to the starting material **3** (76% yield). Exposure of this azophane to the action of bromine in the presence of iron powder in dichloromethane solution resulted in a remarkable substitution reaction: the nitrogen bridge was lost and the pseudo-geminal dibromide **2** was produced in good yield

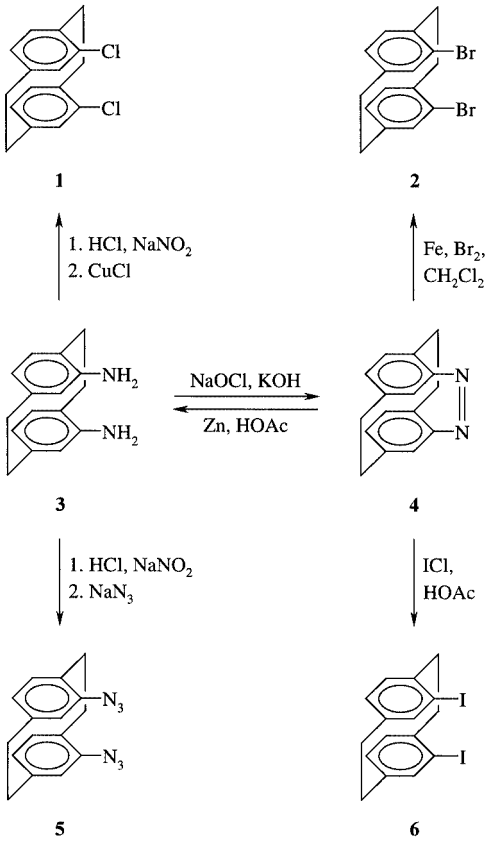

Scheme 1. 4,15-Diamino[2.2]paracyclophane (**3**) as a starting material for pseudo-geminally substituted [2.2]paracyclophanes

(64%). Dibromo[2.2]cyclophanes have been described several times in the literature,[4] but the derivative with the two halogen atoms in pseudo-geminal position has not been available so far. However, this isomer is of particular interest, because it should, in principle, allow the preparation of dimeric organometallic reagents [bis(Grignard reagents), bis(lithio) derivatives], which could be useful for preparative purposes and show interesting structural properties. Similarly, the diiodide **6** was produced (22%) when **4** was treated with iodine monochloride in glacial acetic acid. Again, the structures of **2** and **6** were determined by X-ray structural analysis, and the results are also discussed below.

As far as the mechanism of the deazotization process is concerned, we propose that **4** is initially attacked in *ipso*-fashion at the heteroatom bridge, providing the σ-complex **8**. On expulsion of halide, **8** rearomatizes and is converted into the diazonium salt **9** (Scheme 2). This, in the last step, reacts as a typical representative of this class of compounds and yields the isolated pseudo-geminal dihalide **10**. As far as the production of the diiodide **6** is concerned, it could also be that **4** and the halogenating reagent iodine monochloride first form a mixed [2.2]paracyclophane derivative, in which the chlorine substituent would subsequently be replaced by iodine. Although we attempted to prepare and isolate this mixed intermediate (by changing the concentrations of **4** and ICl) these experiments met with failure.

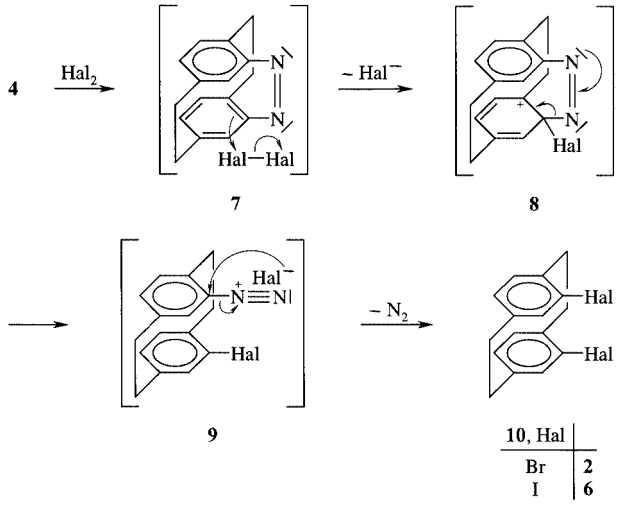

Scheme 2. Mechanism of nitrogen loss from the azocyclophane **4**

The pyrolysis of aliphatic and aromatic azo compounds has been thoroughly investigated,[5] and since **4** can be regarded as a "tied-back" *cis*-azobenzene we thought it interesting to study its high-temperature pyrolytic behavior. As it turned out, the compound is very stable and begins to decompose only at ca. 450 °C, and under these harsh conditions only two defined products, characterized by their spectroscopic data (see Exp. Sect.), could be isolated from the pyrolysate, each in trace amounts: 3,6-dimethylphenanthrene (**13**, 1.5%) and its 9,10-dihydro derivative **14** (1.5%, Scheme 3).

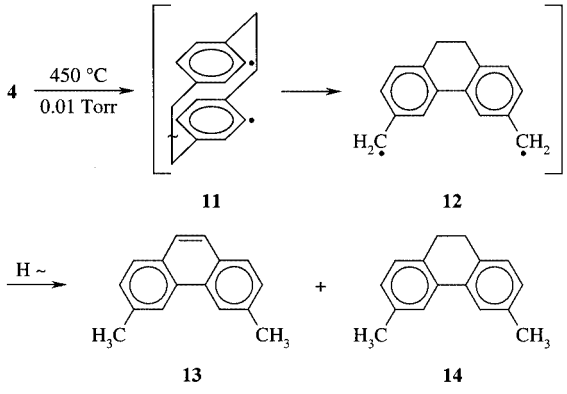

Scheme 3. Flash vacuum pyrolysis of the azocyclophane **4**

To explain the formation of these aromatic hydrocarbons we propose that the diradical **11** is generated in an initial, presumably stepwise, deazotization process. Like [2.2]paracyclophane and several of its derivatives,[6] this intermediate could undergo bridge rupture while simultaneously generating the prerequisite for radical recombination. The double-benzylic diradical **12** thus produced can stabilize itself either by a formal intramolecular hydrogen-transfer process, furnishing **13**, or by intermolecular hydrogen transfer to give **14**. Intermediates such as **12** or reactive species derived from them could in principle also produce dimeric products.

We were, however, unable to identify the corresponding cyclophanes during workup or by mass spectrometric analysis.

To learn more about the reactivity of **4** we first attempted to isomerize the azo compound into its chiral isomer **15** in dichloromethane solution in the presence of catalytic amounts of $AlCl_3$/HCl at 0 °C, the process having previously been carried out successfully for the all-carbon analogue of **15** under the same conditions.[7] However, the starting material was recovered unchanged (Scheme 4).

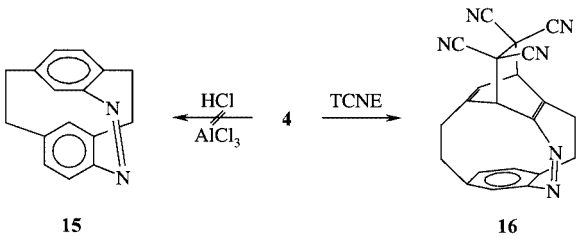

15 **16**

Scheme 4. Attempted isomerization of the azophane **4** and its Diels−Alder cycloaddition

A cycloaddition experiment between **4** and tetracyanoethylene (TCNE) in dichloromethane at room temperature was successful; on mixing of the two compounds the immediate formation of a deep red color was noted and after a few minutes the Diels−Alder adduct **16** began to precipitate. The structure of this adduct, produced in 54% yield, was deduced from its spectroscopic data (see Exp. Sect.) as well as a crystal structure determination (see below). The participation of a benzene ring as the diene component in a [2+4] cycloaddition has been observed several times;[8] however, in none of the previous cases had the addition process been so fast as for **4**.

The Crystal Structures of the New *Pseudo*-Geminally Substituted [2.2]Paracyclophanes

The halo derivatives **1**, **2**, and **6** all crystallize with similar unit cells in $P2_1/n$, but only the bromo derivative **2** and the iodo derivative **6** are isostructural; none of the molecules discussed here possesses imposed crystallographic symmetry (Table 1). All three molecules (Figures 1−3) display general features of [2.2]paracyclophanes, such as the flattened boat configuration of the rings and the lengthened C−C single bonds in the bridges (1.576−1.589 Å). Two effects of the halogen substituents are: first, as noted for, for example, the pseudo-*para*-4,12-dibromo- and -dichloro[2.2]-paracyclophanes,[9] to reduce the ring angles (e.g., C4−C3−C8) at the *ortho* bridgehead carbon atoms to ca. 115°, whereas the corresponding *meta* angles (e.g. C5−C6−C7) remain at the typical cyclophane value of ca. 117°; and secondly, to widen the C−C−C angles from the substituent to the bridge (e.g., C4−C3−C2) to 123−124°, presumably by steric interactions with the bridge hydrogen atoms.[10]

The intramolecular halogen−halogen distances are Cl···Cl 3.4668(5), Br···Br 3.6747(5), and I···I 3.961(2) Å. If these were sterically unfavorable, one would expect some strain to be noticeable. The short non-bonded distances between opposite bridgehead carbon atoms are marginally but consistently greater for the carbon atoms *ortho* to the halogen substituents [2.774, 2.760(2) Å for **1**; 2.776, 2.746(3) Å for **2**; and 2.782, 2.763(4) Å for **6**]. Similarly, the C4···C15 contact increases from 3.166(2) to 3.204(2) and 3.252(4) Å in the order Cl, Br, I. Finally, the interplanar angle between the rings (bridgehead C omitted) increases in the same order, from 2.3 to 3.8 and 5.1°.

The packing of compound **1** consists of layers with a herringbone pattern (Figure 4). Within each layer, generated along the 2_1 screw axis, there are strikingly short and linear intermolecular contacts from hydrogen atoms to the centroids (Cg) of the rings (calculated without the bridgehead atoms): C16−H16···Cg(C4,5,7,8) 2.50 Å, 171° and C2−H2B···Cg(C12,13,15,16) 2.63 Å, 166° (throughout this paper such contacts are quoted for a normalized C−H distance of 1.08 Å).[11] These contacts may reasonably be classified as C−H···π hydrogen bonds;[12] it is, however, surprising that such short contacts are formed by low-acidity donors and chlorine-substituted ring acceptors, which should have a reduced electron density. We have recently pointed out similar interactions, but with longer H··· π distances (up to 2.9 Å), in the layer structures of some [2.2]paracyclophane esters.[10]

An examination of the structures of many simple derivatives of [2.2]paracyclophane reveals that a particular combination of two axis lengths − namely one of ca. 7.5 Å and one of ca. 11.5 Å − is very common; we shall term this the "7,11"-structure. A cursory analysis suggests that the common feature underlying the "7,11"-structure is the herringbone layer (and by implication the C−H···π interaction). The layer dimensions are determined by the size of the [2.2]paracyclophane framework and not by its substituents, which are directed, approximately perpendicularly, away from the layer. The interactions connecting neighboring layers will in general vary depending on the substituents, resulting in different three-dimensional packing and thus different space groups and lengths of the third axis. In **1** the layers are connected through the *n* glide operator by weak C10−H10A···Cl1 hydrogen bonds (2.89 Å, 161°). A more detailed investigation of these packing effects, in which we wish to test whether other packing features can also produce "7,11"-structures in [2.2]paracyclophanes, is in progress.[13] We have ourselves noted C−H···O interactions in such layers and have in some cases subjectively classified them as more important than very long C−H···π interactions;[10] however, we have already pointed out the potential inconsistencies inherent in the subjective ranking of various packing features.[14]

The packing of the isostructural compounds **2** and **6** is illustrated for the iodo derivative **6** in Figures 5 and 6. The "7,11"-type layer is clearly visible in Figure 5; the C−H···π

Table 1. Crystallographic data for compounds **1**, **2**, **4**−**6**, and **16**

	1	**2**	**4**	**5**	**6**	**16**
Empirical formula	$C_{16}H_{14}Cl_2$	$C_{16}H_{14}Br_2$	$C_{16}H_{14}N_2$	$C_{16}H_{14}N_6$	$C_{16}H_{14}I_2$	$C_{22}H_{14}N_6$
M_r	277.17	366.09	234.29	290.33	460.07	362.39
Habit	colorless tablet	colorless, irreg.	yellow prism	colorless plate	colorless prism	colorless tablet
Cryst. size [mm]	0.27×0.25×0.08	0.27×0.24×0.22	0.6×0.4×0.4	0.38×0.32×0.08	0.35×0.21×0.18	0.5×0.4×0.2
Crystal system	monoclinic	monoclinic	orthorhombic	orthorhombic	monoclinic	monoclinic
Space group	$P2_1/n$	$P2_1/n$	$P2_12_12_1$	$P2_12_12_1$	$P2_1/n$	$P2_1/c$
Cell constants:						
a [Å]	7.5506(4)	7.6721(15)	8.020(2)	7.5140(10)	7.662(6)	11.576(2)
b [Å]	11.3311(8)	10.7919(14)	9.279(2)	11.4922(16)	11.069(8)	10.211(3)
c [Å]	15.0074(11)	16.498(3)	15.292(3)	15.989(2)	17.014(15)	15.053(3)
β [°]	99.141(3)	95.380(9)	90	90	97.75(7)	103.39(2)
V [Å^3]	1267.68(15)	1352.0(4)	1138.0(4)	1380.7(3)	1430(2)	767.86(12)
Z	4	4	4	4	4	4
D_x [Mg·m^{-3}]	1.452	1.799	1.368	1.397	2.137	1.391
μ [mm^{-1}]	0.49	6.0	0.08	0.09	4.4	0.09
F(000)	576	720	496	608	864	752
T [°C]	−140	−140	−130	−100	−140	−130
$2\theta_{max}$ [°]	60	60	55	50	60	50
Refl. measured	26112	21509	4153	2742	28762	3212
Refl. independent	3701	3949	1521	1419	4170	3046
Transmissions	0.787−0.962	0.412−0.494	no corr.	no corr.	0.483−0.604	no corr.
R_{int}	0.029	0.024	0.038	0.042	0.023	0.040
Parameters	163	163	163	199	163	253
Restraints	0	0	177	200	0	274
wR (F^2, all refl.)	0.094	0.078	0.139	0.075	0.059	0.150
R [$F > 4\sigma(F)$]	0.032	0.027	0.049	0.039	0.023	0.055
S	1.07	1.08	1.09	0.85	1.08	1.03
max. Δρ [e·Å^{-3}]	0.44	1.5	0.42	0.17	1.8	0.22

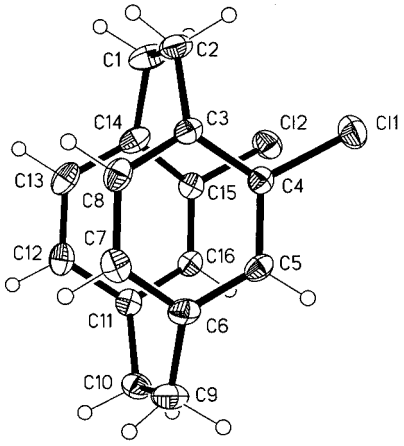

Figure 1. The molecule of compound **1** in the crystal; ellipsoids represent 50% probability levels; hydrogen radii are arbitrary

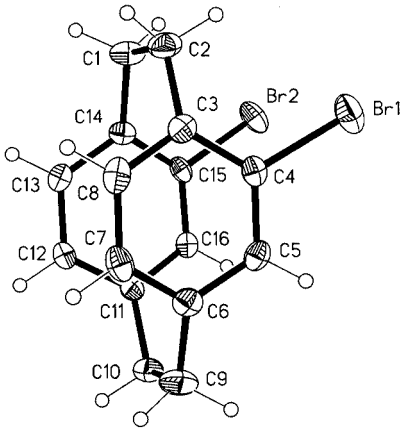

Figure 2. The molecule of compound **2** in the crystal; ellipsoids represent 50% probability levels; hydrogen radii are arbitrary

interactions are C16−H16···Cg(C4,5,7,8) 2.75 Å, 155° and C8−8-H···Cg(C12,13,15,16) 2.80 Å, 160°. Again, the 2_1 operator is involved, although a slight shift in the molecules means that the aromatic hydrogen atom H8 is a donor, rather than the bridge hydrogen atom in **1**. The bromine derivative **2** has C16−H16···Cg(C4,5,7,8) 2.75 Å, 155° and C8−H8···Cg(C12,13,15,16) 2.58 Å (0.22 Å shorter than in **6**), 164°.

The layers in **2** and **6** are linked by two kinds of interaction to form diagonal layers parallel to [101] (Figure 6). Again, it is a subjective decision whether the "7,11" layers or these diagonal layers are the more "important" packing feature. Firstly, there is a weak C−H···Hal hydrogen bond C12−H12···Br1 (2.79 Å, 158°) or C12−H12···I1 (2.97 Å, 150°), generated by the n glide operator, in the region $z \approx 0$. Secondly, there are halogen···halogen interactions [Br1···Br2 3.8072(5), Br2···Br2 3.6223(6) Å or I1···I2 4.026(2), I2···I2 3.921(3) Å] between molecules related by inversion, in the region $z \approx 1/2$. The corresponding C−Hal···Hal angles [°] are 140, 153; 144 (×2) for **2** and 136, 153; 136 (×2) for **6**, corresponding approximately to the "type I" classification.[15]

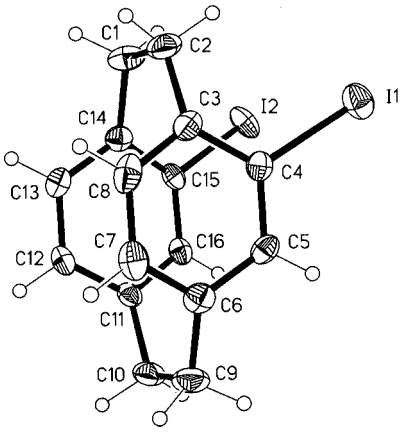

Figure 3. The molecule of compound **6** in the crystal; ellipsoids represent 50% probability levels; hydrogen radii are arbitrary

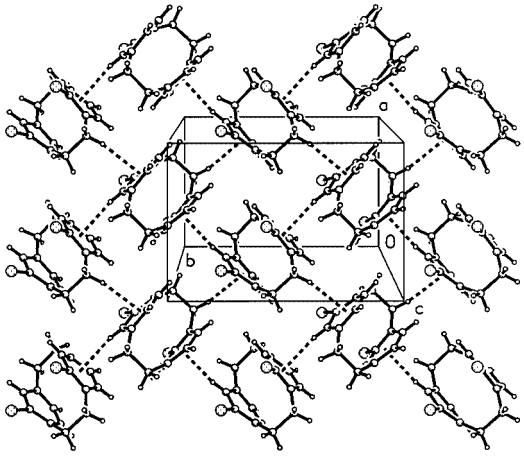

Figure 4. The layer structure of compound **1** seen perpendicular to the *ab* face; hydrogen bonds are shown as broken lines; there are two such layers per *c* axis repeat

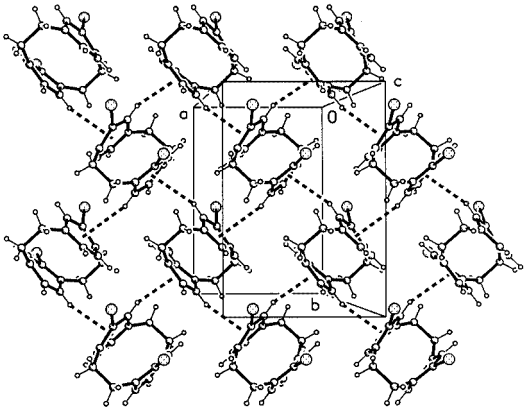

Figure 5. The layer structure of compound **6** seen perpendicular to the *ab* face; hydrogen bonds are shown as broken lines; there are two such layers per *c* axis repeat

The structure of the triply bridged phane **4** (Figure 7) would be expected to show considerable strain; unfortunately, the structure of its hydrocarbon analogue has only been published as a conference abstract[16] and no details are available for comparison. Bond lengths quoted here for **4** have been corrected for libration by use of a rigid-body model;[17] values in Figure 7 are uncorrected. The main feature is the necessarily short diazo bridge, with its N=N bond of 1.272 Å (cf. standard X-ray value of 1.255 Å[18]), associated with a very short non-bonded contact (C4···C15) of 2.504(4) Å (uncorrected); the C−N bond lengths are 1.474 and 1.467 Å, also slightly lengthened from the standard value of 1.431 Å. The C−C bridge bond lengths are 1.592 and 1.607 Å, rather longer than in [2.2]paracyclophanes. Perhaps unexpectedly, the flattened boat description of the six-membered rings is still a fair approximation (r.m.s. deviation of four atoms 0.035 Å, deviations of C3, C6, C11, C14: 0.12, 0.15, 0.15, 0.11 Å), but the interplanar angle is as high as 19.7(1)°. This latter value may be regarded as the main manifestation of strain.

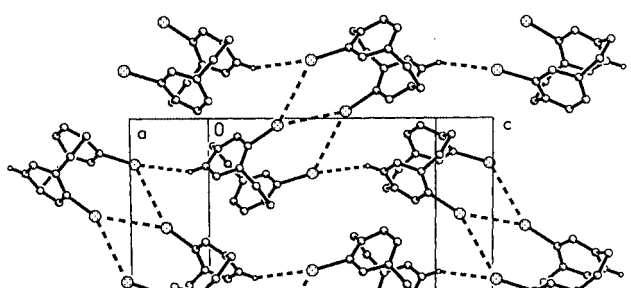

Figure 6. The alternative layer structure of compound **6** seen perpendicular to [101]; hydrogen bonds and I···I interactions are shown as broken lines; H atoms not involved in H bonds are omitted for clarity

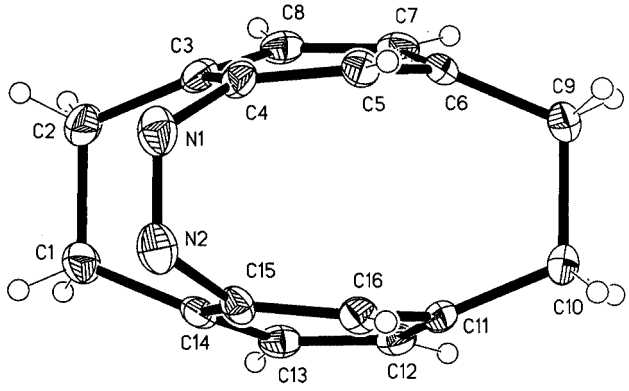

Figure 7. The molecule of compound **4** in the crystal; ellipsoids represent 30% probability levels; hydrogen radii are arbitrary; selected bond lengths [Å] and angles [°]: N1−N2 1.268(4), N1−C4 1.470(3), N2−C15 1.463(4), C1−C2 1.588(4), C9−C10 1.603(4); N2−N1−C4 114.9(2), N1−N2−C15 114.9(2), C4−C3−C8 115.8(3), C3−C4−C5 122.5(3), C5−C6−C7 117.9(2), C12−C11−C16 117.1(2), C13−C14−C15 116.8(2), C14−C15−C16 122.1(3)

The three-dimensional packing of **4** shows no easily recognizable features; the molecules are connected by the three weak hydrogen bonds C16−H16···N1 2.55, C10−H10B···N1 2.77, and C5−H5···N2 2.81 Å (all generated through the 2_1 axis parallel to *b*, and all of acceptable linearity). There are no C−H···π contacts < 3.3 Å.

The structure of the bis(azido) derivative **5** is shown in Figure 8. Its molecular dimensions, some of which are presented in the caption to Figure 8, may be regarded as normal for [2.2]paracyclophanes and azide groups. The latter are essentially coplanar with the rings (deviation 0.32 Å for N3 and 0.14 Å for N6). Surprisingly, the compound is not isostructural with its diisocyanato analogue,[2] although both (and also a urea derivative reported in ref.[2], despite the presence of classical hydrogen bonds) crystallize in the "7,11"-pattern. The C−H···π interactions, however, if such they are, are very long; C13−H13···Cg(C4,5,7,8) 2.81 Å, 161° and C9−H9B···Cg(C12,13,15,16) 3.00 Å, 153°. There are also seven weak C−H···N contacts (three with H10B as donor) with H···N 2.68−2.84 Å, three within the layer and four between layers, but they are far from linear (120−148°). All these contacts must individually represent at best a minor stabilizing influence, but their combined effect could be significant in determining the overall packing. Figure 9 shows the layer structure viewed from the side, showing the contacts between layers.

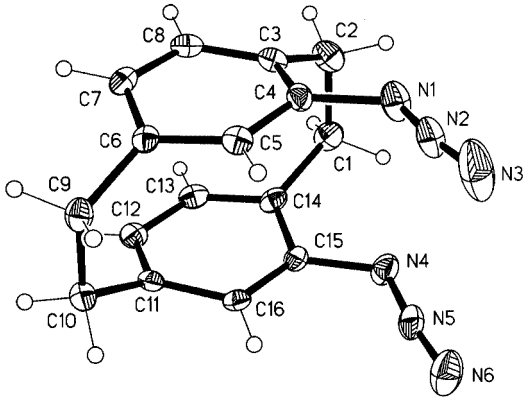

Figure 8. The molecule of compound **5** in the crystal; ellipsoids represent 30% probability levels; hydrogen radii are arbitrary; selected bond lengths [Å] and angles [°]: N1−N2 1.222(2), N2−N3 1.127(4), N4−N5 1.240(4), N5−N6 1.133(4), N1−C4 1.433(4), N4−C15 1.438(4), C1−C2 1.580(5), C9−C10 1.592(4); C4−N1−N2 118.3(3), N1−N2−N3 171.5(4), C15−N4−N5 115.9(3), N4−N5−N6 172.4(4)

The structure of compound **16**, the Diels−Alder addition product of **4**, is shown in Figure 10. The bridge bond lengths (see caption to Figure 10) are relaxed from their increased values in **4** towards more normal values, whereas the bonds involving the new bridge atoms C17 and C18 are long. The ring C11−16 is still a flattened boat, with C11 and C14 lying 0.12 and 0.08 Å out of the mean plane of the other four atoms (r.m.s. deviation 0.02 Å). The non-

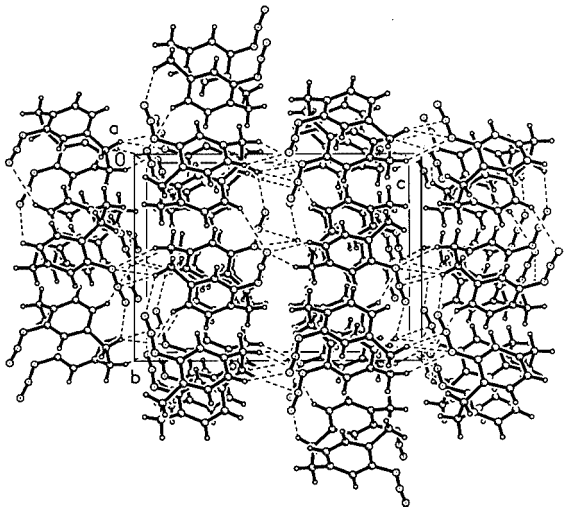

Figure 9. The layer structure of compound **5** seen parallel to the *a* axis; the layers are thus viewed from the side; weak hydrogen bonds C−H···N within and between layers are shown as broken lines

bonded distances across the bridges are C4···C15 2.485(3), C3···C14 2.766(3), and C6···C11 2.765(3) Å.

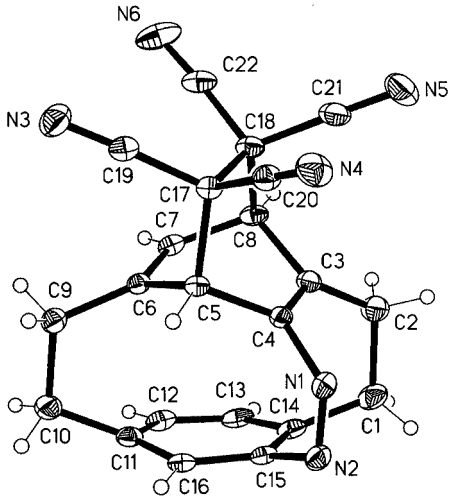

Figure 10. The molecule of compound **16** in the crystal; ellipsoids represent 30% probability levels; hydrogen radii are arbitrary; selected bond lengths [Å] and angles [°]: N1−N2 1.258(3), N1−C4 1.456(3), N2−C15 1.458(3), C1−C2 1.565(4), C9−C10 1.561(3), C5−C17 1.589(3), C17−C18 1.602(3), C8−C18 1.591(3); N2−N1−C4 116.9(2), N1−N2−C15 112.8(2)

In view of the size of the newly inserted TCNE moiety, the "7,11"-packing is no longer to be expected, and indeed is not observed. However, a layer structure based on the 2_1 operator is still formed (Figure 11), and it still involves one short C−H···π interaction to the unaltered ring; C5−H5···Cg(C12,13,15,16) 2.55 Å, 161°. Additionally, there are three weak C−H···N interactions within the layer and three adjoining neighboring layers. As in **5**, most of these are far from linear; by far the shortest are C7−H7···N6 (2.48 Å, 127°) within and C10−H10B···N4 (2.58 Å, 146°) between the layers. All others have H···N

in the 2.7−2.8 Å range and may be considered to play a supporting role in the packing.

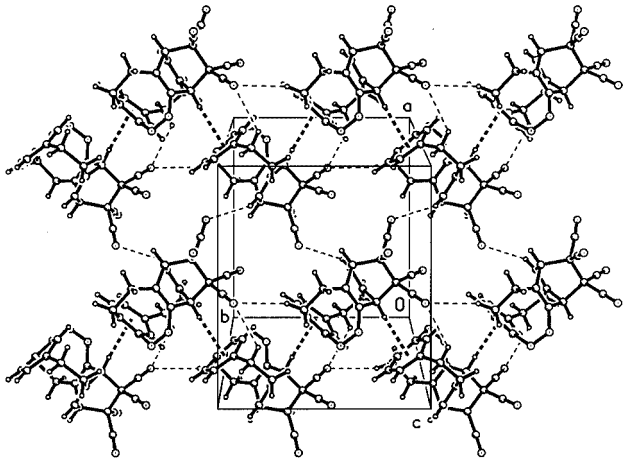

Figure 11. The layer structure of compound **16** seen perpendicular to the *ab* face; weak hydrogen bonds C−H···N are shown as thin and C−H···π as thick broken lines; there are two such layers per *c* axis repeat

The ^{1}H NMR Spectra of the *Pseudo-Geminal* Dihalo[2.2]paracyclophanes and Conformational Equilibria in Solution

We have carefully analyzed the ^{1}H NMR spectra of the homologous series represented by pseudo-geminal difluoro- (**17**),[19] -dichloro- (**1**), -dibromo- (**2**), and -diiodo[2.2]paracyclophane (**6**) because the ^{1}H,^{1}H coupling constants in the CH_2CH_2 bridges contain information about the conformational equilibrium that exists in solution, as we have shown previously for a series of 4-monosubstituted [2.2]paracyclophanes.[20] The difluoro compound **17** (Scheme 5) was available to us from an earlier study.[21]

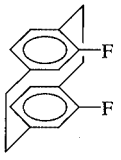

17

Scheme 5

The bridge proton spectra of the dihaloparacyclophanes **1**, **2**, **6**, and **17** each comprise one AA′XX′ spin system for the bridge *ortho* to the halogen atoms and one AA′BB′ spin system for the remote bridge. These spin systems overlap slightly for **1** but strongly for **2**, while they do not overlap in the case of **6** and **17**. The results of the iterative full bandshape analysis are given in Table 2 (chemical shifts) and in Table 3 (coupling constants), and the experimental and calculated spectra of the bridge protons of **1** are shown in Figure 12 to demonstrate their appearance and the quality of the analysis. The relatively large linewidths in the experimental spectrum are due to the multitude of unresolved benzylic coupling constants of magnitudes less than 1 Hz. For **17**, the chemical shifts of the protons of the remote bridge are quite close, giving rise to a very strongly coupled AA′BB′ spectrum in which not enough lines are resolved to define the two vicinal *cis* couplings. However, these are not important with regard to the conformational analysis.

Table 2. ^{1}H NMR chemical shifts of **1**, **2**, **6**, and **17** in $CDCl_3$

	17	**1**	**2**	**6**
δ(1-H*a*)	2.76	2.96	3.03	3.15
δ(1-H*s*)	3.54	3.74	3.72	3.60
δ(5-H)	6.17	6.57	6.79	7.07
δ(7-H)	6.38	6.48	6.51	6.55
δ(8-H)	6.44	6.54	6.53	6.50
δ(9-H*a*)	3.05[a]	3.05	3.04	3.04
δ(9-H*s*)	3.02[a]	2.99	2.98	2.97

[a] Assignments are interchangeable.

Table 3. Spin,spin coupling constants involving ^{1}H in **1**, **2**, **6**, and **17** and involving ^{19}F in **17**

	17	**1**	**2**	**6**
J(1-H*a*,1-H*s*) = J_{gem}	−13.6	−13.6	−13.6	−13.7
J(1-H*a*,2-H*a*) = J_{cis}[a]	10.2	10.5	10.5	10.4
J(1-H*a*,2-H*s*) = J_{trans}	4.2	4.1	4.1	4.2
J(1-H*s*,2-H*s*) = J_{cis}[a]	9.7	10.1	10.1	9.9
J(5-H,7-H)	1.8	1.8	1.8	1.7
J(5-H,8-H)	0.4	n.r.[b]	n.r.[b]	n.r.[b]
J(7-H,8-H)	7.8	7.8	7.7	7.7
J(5-H,F)	11.4			
J(7-H,F)	−0.9			
J(8-H,F)	8.2			
$J_{F,F}$	13.8			
J(9-H*a*,9-H*s*) = J_{gem}	−13.4 ± 0.2	−13.3	−13.4	−13.4
J(9-H*a*,10-H*a*) = J_{cis}[a]	n.d.[c]	10.4	10.6	10.3
J(9-H*a*,10-H*s*) = J_{trans}	14.3 ± 0.2	4.2	4.1	4.3
J(9-H*s*,10-H*s*) = J_{cis}[a]	n.d.[c]	10.6	10.7	10.5

[a] In principle, the two J_{cis} values in the AA′XX′ or AA′BB′ spin systems cannot be assigned individually. [b] Not resolved. [c] Coupling constant not properly defined due to insufficient number of observed transitions.

The aromatic protons of **17** are part of a complicated AA′BB′CC′XX′ spin system, due to the existence of considerable through-space ^{19}F,^{19}F coupling causing magnetic nonequivalence. To reproduce the 5-H/16-H multiplet at δ = 6.17 ppm (Figure 13), *para*-F,H and -H,H couplings of −0.9 Hz and 0.4 Hz (the latter unresolved), respectively, were required. The iterative analysis converged on a $|J_{F,F}|$ value of 13.8 Hz, in good agreement with our previous result of 13.7 Hz obtained from the ^{13}C satellites in the ^{1}H-decoupled ^{19}F NMR spectrum.[22]

In [2.2]paracyclophane (**18**, R = H) in solution, there is a degenerate equilibrium between the two skew conformations **18A** and **18B** (Scheme 6). These are separated by a

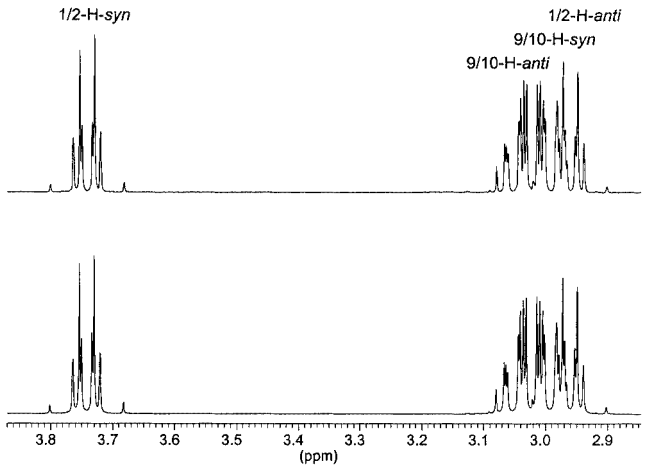

Figure 12. 400 MHz ^{1}H NMR spectrum of the bridge proton region of **1** in $CDCl_3$ solution; experimental (top), iteratively fitted (bottom)

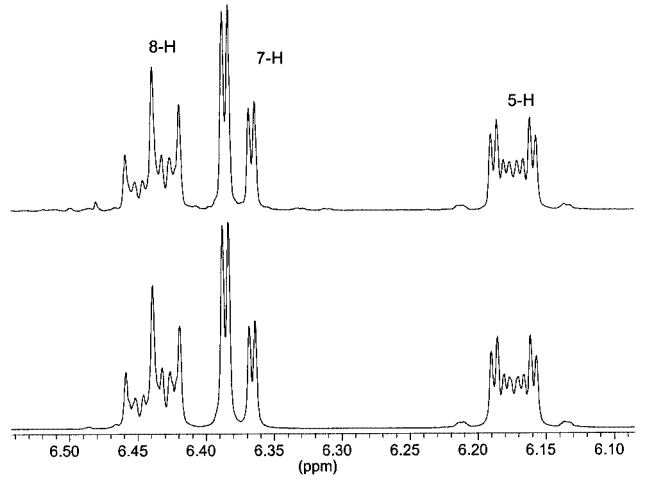

Figure 13. 400 MHz ^{1}H NMR spectrum of the aromatic region of **17** in $CDCl_3$ solution; experimental (top), iteratively fitted (bottom)

low energy barrier (estimated to be 2.5 kJ·mol^{-1} by ab initio MO calculation[23]) and interconvert rapidly at room temperature by a twisting movement about the axis joining the centers of the two aromatic rings. The conformational equilibrium of **18** becomes biased when a substituent is introduced in the 4-position.[20] The bias is such as to favor conformation **18B**, in which the *syn*-C−H bond at the *ortho*-bridge carbon atom C-2 is twisted away from the plane of the adjacent aromatic ring in order to avoid unfavorable nonbonding interactions between 2-H*s* and the substituent. At the same time, the *anti*-C−H bond of the *ortho*-bridge carbon atom is twisted towards the aromatic plane. This was deduced from the decrease in one *trans* coupling constant, *J*(1-H*a*,2-H*s*), and the increase in the other, *J*(1-H*s*,2-H*a*), whereas both *cis* coupling constants, *J*(1-H*s*,2-H*s*) and *J*(1-H*a*,2-H*a*), are more or less unaffected. The rationale behind this is that the Karplus function describing the dependence of vicinal coupling constants upon the H−C−C−H dihedral angle α is symmetrical about 0° but not about 120°. It had indeed been found that the larger the spatial requirement of the substituent at C-4, the larger *J*(1-H*s*,2-H*a*) and the smaller *J*(1-H*a*,2-H*s*) becomes, indicating the increasing bias of the equilibrium toward **18B**. Extreme values − 7.2 Hz and 1.5 Hz, respectively − had been observed for **18** (R = NO_2), compared with the value of 4.1 Hz for **18** (R = H).

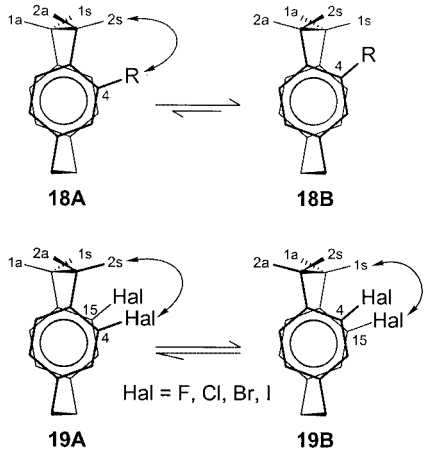

Scheme 6. Equilibria between the twisted conformations **18A** and **18B** of 4-substituted [2.2]paracyclophanes and between conformations **19A** and **19B** of 4,15-disubstituted [2.2]paracyclophanes; unfavorable nonbonding interactions are indicated by double-headed arrows

Comparison of aromatic monosubstitution (**18**) to pseudo-geminal disubstitution (**19**) makes it clear that evasion of the unfavorable 2-H*s*/4-Hal interaction in **19A** by shifting the equilibrium towards **19B** is no longer helpful because, as the 2-H*s*/4-Hal interaction decreases, the analogous 1-H*s*/15-H interaction correspondingly increases (Scheme 6). No alleviation of the nonbonding strain can hence be expected from a shift of the conformational equilibrium. Inspection of the vicinal *trans* coupling constants in Table 3 shows that these are in fact constant throughout the halogen series (4.2 ± 0.1 Hz) and not affected by the size of the halogen substituents. Moreover, these coupling constants have the same value, within experimental error, as in paracyclophane itself (4.1 Hz). This shows that **19A** and **19B** are populated in a 1:1 ratio. The Dreiding molecular models that we used to represent the conformers under discussion are not well suited for this purpose because they are highly strained. It was therefore not immediately obvious that **19A** and **19B** are enantiomorphic; only molecular modeling made this clear beyond doubt. Thus, the experimentally observed coupling constants are indeed those expected as the consequence of the molecular symmetry, provided there is no direct electronic influence of the halogen atoms on the vicinal $J_{H,H}$.

Experimental Section

General Remarks: The instrumentation used for structure determination has been described previously.[1,2] The ^{13}C NMR spectra

of **1**, **2**, and **6** were assigned by 2D correlation techniques (HSQC, HMBC). The ^{1}H NMR spectra of **1**, **2**, **6** and **17** were analyzed by the full lineshape method with the program Win-DAISY 4.0 (Bruker-Franzen Analytik, Bremen).[24]

4,15-Dichloro[2.2]paracyclophane (1): 4,15-Diamino[2.2]paracyclophane (**3,** 0.100 g, 0.42 mmol) was dissolved in concd. HCl (10 mL), the solution was cooled to 0 °C with an ice bath whilst stirring, and sodium nitrite (0.390 g, 5.65 mmol), dissolved in water (5 mL) and cooled to 0 °C, was added dropwise. The diazonium salt solution produced was added, also at 0 °C, to a solution of cuprous chloride (0.800 g, 8.08 mmol) in concd. HCl (5 mL). The resulting mixture was allowed to warm to room temp. and to stand for 3 h, and was then heated with a water bath at 70 °C for 30 min. The product mixture was extracted with diethyl ether, and the diethyl ether phase was washed with satd. bicarbonate solution and brine solution, and dried with anhydrous $MgSO_4$. After solvent evaporation, the crude product was column-chromatographed on silica gel with 5% diethyl ether in pentane, providing **1** as a colorless solid (0.040 g, 35%). Recrystallisation from $CHCl_3$/pentane gave colorless single crystals (m.p. 186 °C, plates) used for X-ray analysis (see below). ^{1}H NMR: see Tables 2 and 3. ^{13}C NMR (100.6 MHz, $CDCl_3$, int. TMS): δ = 32.2 (C-1, C-2), 34.7 (C-9, C-10), 131.7 (C-7, C-12), 133.0 (C-5, C-16), 134.9 (C-4, C-15), 135.3 (C-8, C-13), 136.7 (C-3, C-14), 140.9 (C-6, C-11) ppm. IR (KBr): $\tilde{\nu}$ = 3444 cm^{-1}, 3043, 3014, 2963, 2934, 2853, 1587, 1482, 1435, 1395, 1261, 1111, 1043, 838, 708, 698. UV/Vis ($CHCl_3$): λ_{max} (log ε) = 328 nm (1.22), 342 (1.18), 358 (1.04, sh). MS (EI, 70 eV): *m*/*z* (%) = 278 (8), 276 (14) [M$^+$], 202 (2), 172 (3), 140 (30), 138 (100), 103 (22), 77 (14), 63 (4), 51 (8). HRMS: calcd. 276.047255; found 276.04729.

4,15-Diazido[2.2]paracyclophane (5): 4,15-Diamino[2.2]paracyclophane (**3**, 0.238 g, 1.0 mmol) was dissolved in hydrochloric acid [prepared from 0.146 g (4 mmol) of concd. hydrochloric acid and 10 mL of water], and the solution was cooled to −10 °C. A solution of sodium nitrite (0.276 g, 4 mmol) in water (10 mL) was added dropwise whilst stirring for 1 h, followed by additional stirring for 1 h. To remove insoluble material, the diazonium salt solution was filtered and the filtrate was cooled to −5 °C in an ice bath. A solution of sodium azide (0.260 g, 4 mmol) in water (10 mL) was added slowly whilst stirring, and after 1 h the formed precipitate was removed by filtration. The crude product was washed with water, dried over phosphorus pentoxide, and dissolved in dichloromethane (10 mL), and the solution was fractionated by thick layer chromatography on silica gel with pentane/dichloromethane (5:1, v/v) to yield 0.091 g (31%) of **5**, m.p. 138−139 °C. ^{1}H NMR (400.1 MHz, $CDCl_3$, int. TMS): δ = 2.66−2.70 (m, 2 H), 2.94−3.40 (m, 4 H), 3.35−3.40 (m, 2 H), 6.17 (d, *J* = 1.6 Hz, 2 H), 6.31 (dd, *J* = 7.7, 1.6 Hz, 2 H), 6.38 (d, *J* = 7.7 Hz, 2 H) ppm. ^{13}C NMR (100.6 MHz, $CDCl_3$, int. TMS): δ = 30.4, 34.9 (2 × CH_2), 122.9, 129.9, 131.1, 135.6, 138.2, 141.3 (6 × arom. C) ppm. IR (KBr): $\tilde{\nu}$ = 3029 cm^{-1}, 2894, 2875, 2853, 2110 (N_3). MS (EI, 70 eV): *m*/*z* (%) = 290 (70) [M$^+$], 255 (24), 234 (100), 219 (40), 206 (66), 130 (24), 116 (46), 90 (34), 77 (22), 63 (16), 51 (18). $C_{16}H_{14}N_6$ (290.3): calcd. C 66.19, H 4.86, N 28.95; found C 65.79, H 5.05, N 28.69.

4,15-Azo[2.2]paracyclophane (4): 4,15-Diamino[2.2]paracyclophane (**3**, 0.119 g, 0.50 mmol) was added to a solution of potassium hydroxide (0.5 g, 9 mmol) in ethanol (95%). The reaction mixture was cooled to −8 °C, and a freshly prepared aqueous sodium hypochlorite solution (15 mL) was added. After 30 min of stirring at this temperature, the mixture was poured into 100 mL of ice-cold water. The product was extracted with dichloromethane, the organic phases were combined and dried with $MgSO_4$, the solvent was removed in vacuo, and the remaining solid was purified by silica gel chromatography with dichloromethane. Recrystallization from dichloromethane gave **4** as yellow plates (0.112 g, 96%), m.p. 235 °C. ^{1}H NMR (400.1 MHz, $CDCl_3$, int. TMS): δ = 2.46−2.50 (m, 2 H), 2.83−2.89 (m, 2 H), 2.96−3.05 (m, 2 H), 3.09−3.15 (m, 2 H), 5.60 (d, *J* = 1.7 Hz, 2 H), 6.31 (d, *J* = 8.0 Hz, 2 H), 6.35−6.37 (dd, *J* = 8.0, 1.7 Hz, 2 H) ppm. ^{13}C NMR (100.6 MHz, $CDCl_3$, int. TMS): δ = 31.1, 35.9 (2 × CH_2), 127.3, 129.7, 130.8, 134.1, 140.9, 141.1 (6 × arom. C) ppm. IR (KBr): $\tilde{\nu}$ = 3041 cm^{-1}, 3029, 2964, 2930, 2891, 2851, 1584. UV/Vis (CH_2Cl_2): λ_{max} (log ε) = 222 nm (1.59), 250 (1.50), 268 (1.22), 280 (1.10), 408 (0.62). MS (EI, 70 eV): *m*/*z* (%) = 234 (100) [M$^+$], 206 (50), 191 (80), 178 (60), 165 (30), 152 (20), 128 (10), 115 (10), 102 (10), 89 (20), 77 (22), 63 (100), 51 (12). $C_{16}H_{14}N_2$ (234.3): calcd. C 82.02, H 6.02, N 11.95; found C 81.79, H 6.03, N 11.78.

Reduction of 4 to 3: Compound **4** (0.234 g, 1.0 mmol) was added to a suspension of zinc (0.100 g, 1.53 mmol) in glacial acetic acid (30 mL), and the mixture was stirred for 1 h at room temp. The zinc dust was removed by filtration, the solvent was removed in vacuo, and the remaining residue was purified by silica gel chromatography with ethyl acetate. After solvent evaporation, the crude diamine **3** was recrystallized from ethanol to yield 0.180 g (76%), identical in its spectroscopic properties with an authentic sample.

4,15-Dibromo[2.2]paracyclophane (2): Iron powder (0.150 g, 2.77 mmol) was added to a solution of 4,15-azo[2.2]paracyclophane (**4**, 0.150 g, 0.64 mmol) in anhydrous CH_2Cl_2 (20 mL), and the reaction mixture was cooled to 0 °C. A solution of bromine (0.103 g, 1.28 mmol) in anhydrous CH_2Cl_2 (15 mL) was added dropwise with stirring. The reaction was allowed to continue for 30 min at 0 °C. The residual iron powder was filtered off and the solvent was evaporated. The crude black solid was chromatographed on silica gel with 5% CH_2Cl_2 in pentane to give **2** (0.150 g, 64%) as a colorless solid. Recrystallization from $CHCl_3$/pentane gave colorless plates (m.p. 180 °C), used for X-ray analysis (see below). ^{1}H NMR: see Tables 2 and 3. ^{13}C NMR (100.6 MHz, $CDCl_3$, int. TMS): δ = 34.6 (C-1, C-2), 34.7 (C-9, C-10), 125.1 (C-4, C-15), 132.3 (C-7, C-12), 135.1 (C-8, C-13), 135.7 (C-5, C-16), 138.5 (C-3, C-14), 140.9 (C-6, C-11) ppm. IR (KBr): $\tilde{\nu}$ = 3442 cm^{-1}, 3068, 3021, 3010, 2958, 2931, 1891, 1582, 1537, 1475, 1466, 1389, 1189, 1034, 950, 903, 866 831, 803, 705, 644. MS (EI, 70 eV): *m*/*z* (%) = 368 (18), 366 (30), 364 (16) [M$^+$], 322 (8), 202 (6), 185 (10), 184 (98), 182 (100), 138 (12), 103 (33), 77 (38), 51 (16), 44 (30). HRMS: calcd. 363.94623; found 363.94455. $C_{16}H_{14}Br_2$ (366.1): calcd. C 52.49, H 3.85; found C 52.28, H 3.77.

4,15-Diiodo[2.2]paracyclophane (6): 4,15-Azo[2.2]paracyclophane (**4**, 0.200 g, 0.85 mmol) was dissolved in glacial acetic acid (ca. 30 mL) and the mixture was cooled in an ice/water bath whilst stirring. Iodine monochloride (0.153 g, 0.939 mmol) was added, the ice bath was removed, and the stirring was continued at room temp. for 3 h. The crude mixture was repeatedly extracted with diethyl ether. The diethyl ether phase was washed with water, saturated $NaHCO_3$ solution, and brine solution, and dried with $MgSO_4$. The solvent was evaporated in a rotary evaporator and the residue was chromatographed on silica gel with 20% CH_2Cl_2 in pentane, giving rise to **6** as a colorless solid (0.086 g, 22%). Single crystals (plates, m.p. 239 °C) for X-ray analysis (see below) were obtained by recrystallization from CH_2Cl_2/pentane. ^{1}H NMR: see Tables 2 and 3. ^{13}C NMR (100.6 MHz, $CDCl_3$, int. TMS): δ = 34.7 (C-9, C-10), 38.9 (C-1, C-2), 99.8 (C-4, C-15), 133.4 (C-7, C-12), 133.9 (C-8, C-13), 140.7 (C-6, C-11), 141.8 (C-5, C-16), 142.5 (C-3, C-14) ppm. IR (KBr): $\tilde{\nu}$ = 3418 cm^{-1}, 3029, 2954, 2927, 2886, 2850, 1575, 1532, 1467, 1460, 1446, 1430, 1385, 1024, 901, 862, 823, 813, 805, 705,

656, 639. UV/Vis (acetonitrile): λ_{max} (log ε) = 228 nm (2.25), 238 (2.18), 250 (1.82). MS (EI, 70 eV): *m*/*z* (%) = 460 (16) [M^+], 368 (8), 264 (8), 230 (100), 189 (20), 138 (8), 103 (10), 77 (12), 57 (12). HRMS: calcd. 459.918504; found 459.91783.

Pyrolysis of 4: In a pyrolysis apparatus consisting of a preheating zone and the actual pyrolysis tube (quartz), compound **4** (0.300 g, 1.28 mmol) was sublimed at 200 °C and 0.01 Torr into the hot zone, which was maintained at 450 °C. Unfortunately, a large fraction of the substrate condensed between the two temperature zones. However, a pyrolysate could be obtained, and was trapped in a liquid nitrogen cooled trap, its TLC (dichloromethane/pentane, 4:1, v/v) showing that it consisted of two components, 3,6-dimethylphenanthrene (**13**, 4 mg, 1.5%) and 9,10-dihydro-3,6-dimethylphenanthrene (**14**, 4 mg, 1.5%), both known compounds, the structures of which were determined by NMR and GC/MS analysis. **13:** ^{1}H NMR (400.1 MHz, $CDCl_3$, int. TMS): δ = 2.63 (s, 6 H, 2 × CH_3), 7.41 (br. d, *J* = 8.1 Hz, 2 H), 7.64 (s, 2 H), 7.77 (d, *J* = 8.1 Hz, 2 H), 8.47 (br. s, 2 H) ppm. ^{13}C NMR (100.6 MHz, $CDCl_3$, int. TMS): δ = 22.1, 122.3, 125.7, 128.1, 128.3, 130.0, 130.4, 135.8. MS (EI, 70 eV): m/*z* (%) = 206 (100) [M^+], 191 (30), 101 (12), 89 (8), 76 (7) ppm. **14:** ^{1}H NMR (400.1 MHz, $CDCl_3$, int. TMS): δ = 2.40 (s, 6 H, 2 × CH_3), 2.81 (s, 4 H, 2 × CH_2), 7.04 (br. d, *J* = 7.6 Hz, 2 H), 7.12 (d, *J* = 7.6 Hz, 2 H), 7.57 (s, 2 H) ppm. ^{13}C NMR (100.6 MHz, $CDCl_3$, int. TMS): δ = 21.4, 28.8, 124.3, 127.9, 134.4, 134.5, 136.2 ppm; one signal missing due to signal overlap. MS (EI, 70 eV): *m*/*z* (%) = 208 (98) [M^+], 193 (100), 178 (50), 165 (64), 152 (16), 95 (10), 76 (16).

Diels–Alder Addition of 4: A solution of **4** (0.120 g, 0.51 mmol) in anhydrous dichloromethane (10 mL) was added to a solution of tetracyanoethylene (0.065 g, 0.51 mmol) in anhydrous dichloromethane (10 mL). The color of the reaction mixture immediately changed to red, and after 5 min a precipitate began to form. This was removed by filtration, washed several times with dichloromethane, and dried over phosphorus pentoxide to give brown crystals of **16** (100 mg, 54%), m.p. 154–155 °C. ^{1}H NMR (400 MHz, [D_6]acetone, int. TMS): δ = 2.05–2.18 (m, 1 H), 2.27–2.45 (m, 1 H), 2.50–2.75 (m, 5 H), 3.10–3.29 (m, 1 H), 4.30–4.50 (dd, *J* = 7.6, 1.8 Hz, 1 H), 5.50 (d, *J* = 1.8 Hz, 1 H), 5.65 (d, *J* = 7.6 Hz, 1 H), 6.50 (d, *J* = 1.6 Hz, 1 H), 6.89–6.91 (dd, *J* = 7.8, 1.6 Hz, 1 H), 7.06 (d, 1 H, 7.8 Hz) ppm. ^{13}C NMR (100 MHz, [D_6]acetone, int. TMS): δ = 31.5, 32.8, 33.1, 33.2 (4 × CH_2), 45.1, 45.6 (2 × bridgeheads), 53.0, 55.1 (2 × *C*$(CN)_2$], 113.0, 113.1, 113.2, 113.4 (4 × CN), 120.2 (=CH), 128.0, 130.3, 130.6, 130.8, 131.5, 132.0, 132.5, 134.9, 142.6 (olefinic and arom. C) ppm. IR (KBr): $\tilde{\nu}$ = 3087 cm^{-1}, 3039, 2933, 2865, 2246, 2203 (CN), 1565 (N=N). MS (EI, 70 eV): *m*/*z* (%) = 362 (60) [M^+], 258 (100), 205 (20), 190 (30), 164 (42), 102 (28), 71 (20), 53 (10). $C_{22}H_{14}N_6$ (362.39): calcd. C 72.91, H 3.89, N 23.19; found C 72.75, H 3.92, N 22.96.

X-ray Structure Determinations: Numerical details are presented in Table 1. Data collection and reduction: crystals were mounted in inert oil on glass fibers and transferred to the cold gas stream of the diffractometer (**1**, **2**, **6**: Bruker SMART 1000 CCD; **4**, **16**: Stoe STADI-4; **5**: Siemens P4, with appropriate low-temperature attachments). Measurements were performed with monochromated Mo-K_α radiation. An absorption correction for compounds **1**, **2**, and **6** was performed by use of the SADABS program. Structure solution and refinement: The structures were solved by direct methods and refined anisotropically against F^2 (G.M. Sheldrick, *SHELXL-97*, University of Göttingen). H atoms were included with a riding model. For compounds **4** and **5**, which by chance crystallize in chiral space groups, the absolute structure could not be determined and Friedel opposite reflections were therefore merged. For the more weakly diffracting compounds **4**, **5**, and **16**, a system of restraints to displacement factor components was employed to improve refinement stability. CCDC-186258 (**1**), -186259 (**2**), -186260 (**4**), -186261 (**5**), -186262 (**6**), and -186263 (**16**) contain the supplementary crystallographic data for this paper. These data can be obtained free of charge at www.ccdc.cam.ac.uk/conts/retrieving.html [or from the Cambridge Crystallographic Data Centre, 12 Union Road, Cambridge CB2 1EZ, UK; Fax: (internat.) + 44-1223/336-033; E-mail: deposit@ccdc.cam.ac.uk].

Acknowledgments

We are grateful to the Ministry of Higher Education of the Arabian Republic of Egypt (Mission Department) and the Fonds der Chemischen Industrie for the support of our studies and to Professor Waldemar Adam (University of Würzburg) for helpful discussions. We thank Ms. Petra Holba-Schulz for measuring numerous NMR spectra and Dr. Jörg Grunenberg for help with molecular modeling. We are also obliged to one referee for his proposals on the mechanism of the deazotization process of **4**.

[1] R. Savinsky, H. Hopf, I. Dix, P. G. Jones, *Eur. J. Org. Chem.* **2001**, 4595–4606.
[2] H. Zitt, I. Dix, H. Hopf, P. G. Jones, *Eur. J. Org. Chem.* **2001**, 2298–2307.
[3] In a different project we are concerned with the synthesis of heteroatom-bridged cyclophanes and will report shortly on the preparation of cyclophanes possessing sulfur bridges (H. Hopf, H. Christoph, unpublished results; cf. H. Christoph, Ph.D. thesis, Braunschweig, **2001**).
[4] [4a] H. J. Reich, D. J. Cram, *J. Am. Chem. Soc.* **1969**, *91*, 3527–3533. [4b] G. C. Bazan, W. J. Oldham, Jr., R. L. Lachicotte, S. Tretiak, V. Chernyak, S. Mukamel, *J. Am. Chem. Soc.* **1989**, *120*, 9188–9204.
[5] Review: P. S. Engel, *Chem. Rev.* **1980**, *80*, 99–150; for the thermal decomposition of azobenzene see: D. Barton, M. Hodgett, P. Skirving, M. Whelton, K. Winter, C. Vardy, *Can. J. Chem.* **1983**, *61*, 1712–1718; M. F. Budyka, M. M. Kantor, *Izv. Akad. Nauk, Ser. Khim.* **1993**, 1562–1564; *Russ. Chem. Bull.* **1993**, *42*, 1495–1497.
[6] W. R. Roth, H. Hopf, A. de Meijere, F. Hunold, S. Börner, M. Neumann, T. Wasser, C. Mlynek, *Liebigs Ann. Chem.* **1996**, 2141–2154.
[7] K. Broschinski, Ph.D. thesis, Braunschweig, **1984**.
[8] For a summary of the literature see: H. Hopf, C. Marquard in *Chemical Implications of Strain, Strain Release in Aromatic Compounds: The [2$_n$]Cyclophanes* (Eds.: A. de Meijere, S. Blechert), Reidel Publishing Comp., **1989**; NATO ASI Ser., Ser. C, **1989**, *273*, 297–332.
[9] S. V. Lindeman, Y. T. Struchkov, V. N. Guryshev, *Bull. Acad. Sci. USSR.* **1986**, *35*, 1825–1827.
[10] P. G. Jones, J. Hillmer, H. Hopf, *Acta Crystallogr., Sect. C* **2002**, *58*, 301–304.
[11] T. Steiner, *Acta Crystallogr., Sect. B* **1998**, *54*, 456–463.
[12] N. N. L. Madhavi, A. K. Katz, H. L. Carrell, A. Nangia, G. R. Desiraju, *Chem. Commun.* **1997**, 1953–1954; G. R. Desiraju, T. Steiner, *The Weak Hydrogen Bond*, Oxford, University Press, **1999**.
[13] P. G. Jones, I. Dix, manuscript in preparation.
[14] M. Freytag, P. G. Jones, *Z. Naturforsch., Teil B* **2001**, *56*, 889–896.
[15] V. R. Pedireddi, D. S. Reddy, B. S. Gould, D. C. Craig, A. D. Rae, G. R. Desiraju, *J. Chem. Soc., Perkin Trans. 2* **1994**, 2353–2360.

[16] R. Weiss, K. N. Trueblood, *Am. Crystallogr. Assoc. Abstr. Papers (Summer)* **1974**, 251.
[17] V. Schomaker, K. N. Trueblood, *Acta Crystallogr., Sect. B* **1968**, *24*, 63−76.
[18] F. H. Allen, O. Kennard, D. G. Watson, L. Brammer, A. G. Orpen, R. Taylor, *J. Chem. Soc., Perkin Trans. 2* **1987**, S1−S19.
[19] X. Huang, F. Qu, Z. Li, *J. Fluorine Chem.* **1988**, *40*, 33−39.
[20] L. Ernst, *Liebigs Ann.* **1995**, 13−17.
[21] L. Ernst, K. Ibrom, *Magn. Reson. Chem.* **1997**, *35*, 868−876.
[22] L. Ernst, K. Ibrom, *Angew. Chem.* **1995**, *107*, 2010−2012; *Angew. Chem. Int. Ed. Engl.* **1995**, *34*, 1881−1882.
[23] D. Henseler, G. Hohlneicher, *J. Phys. Chem. A* **1998**, *102*, 10828−10833.
[24] U. Weber, H. Thiele, *NMR Spectroscopy: Modern Spectral Analysis*, Wiley-VCH, Weinheim, **1998**.

Received July 18, 2002
[O02399]